Kinetic Fractionation of Antimony Isotopes during Reduction by Sulfide

Hannah J. Veldhuizen[1,*,‡], *Joel S. MacKinney,*[1,†], *and Thomas M. Johnson*[1,‡]

Department of Earth Science and Environmental Change, University of Illinois Urbana-Champaign, Champaign, IL, 61801, USA

Keywords: Antimony, isotope, redox, sulfide, fractionation

Stable isotope ratios of antimony (Sb) in the environment can provide valuable information on sources and processes such as redox transformations. To investigate the fractionation when Sb(V) is chemically reduced by sulfide to Sb(III), experiments with 0.008 to 0.01 mM Sb(V) and 0.009 to 6 mM sulfide at a pH of 1 to 8 were performed. Experiments at pH 1 to 6 precipitated Sb_2S_3, while at pH 7 to 8 Sb(III) remained in solution. The Sb(III) product was enriched in the lighter isotope. The isotopic fractionation ($\varepsilon \approx \delta_{\text{instantaneous product}} - \delta_{\text{reactant}}$) for the pH 1 experiment was -1.42 ± 0.04‰ while the pH 5 to 8 experiments ranged from -0.46 ± 0.04‰ to -0.62 ± 0.04‰. The small magnitude of fractionation observed in experiments at circumneutral pH may decrease the utility of Sb isotope measurement as reduction indicators in natural systems, as adsorption of Sb has been shown to fractionate isotopes in the same direction and similar magnitude (up to 1.14‰) (Wasserman, 2020; Zhou et al., 2023).

1. INTRODUCTION

Antimony (Sb) is a toxic and carcinogenic metalloid that enters the environment through both natural processes (weathering, volcanic eruptions) and anthropogenic input. Anthropogenic input includes mining and processing of antimony-containing ores and the production of antimony metal.[1] Sulfide minerals such as stibnite are commonly mined for Sb extraction, and the tailings left behind from this process are vulnerable to leaching.[2] Monitoring of Sb contamination in the natural waterways and drinking water will be essential to maintain clean water during mining operations. The maximum contaminant level of Sb in drinking water is set at 6 μg/L by the United States Environmental Protection Agency[3], and the average Sb concentration in drinking water near the Xikuangshan Sb mine in China was found to be 53.6 ± 4.7 μg/L.[4] Despite Sb's increasing use, limited studies exist on its mobility, redox geochemistry, and toxicity.

Sb is commonly found as either Sb(V) (+5 valence) or Sb(III) (+3 valence) in the natural environment. Redox reactions can mobilize or immobilize certain potentially toxic metalloids like Sb. The redox properties of Sb are a driving factor for many of the reactions this element participates in, such as adsorption and dissolution. While Sb(V) is more thermodynamically stable than Sb(III) in oxic environments, Sb redox reactions in anoxic conditions are lacking thermodynamic data.[5] Anoxic zones in groundwater aquifers are areas where Sb should be closely monitored because the toxicity of Sb is greatest for Sb(III), followed by Sb(V), and least for organic antimony species.[3] A variety of abiotic chemical species have been shown to reduce Sb(V) such as, sulfide, Fe(II) containing minerals, and KI.[5] In addition, several studies have demonstrated redox transformations by Sb-reducing microbiota.[6–8]

Stable isotope ratios of elements in the environment can provide valuable information on sources and geochemical reactions. Stable isotopes can be used to determine the extent of certain

reactions in an aquifer, often with better accuracy than concentrations and without complications caused by dilution.[9] For example, if a decrease in Sb concentrations over space or time is identified in groundwater, the cause could be dilution with clean water, adsorption onto solids, or precipitation by reduction. An accompanying isotope measurement could qualitatively identify reduction as the cause of the decreased Sb concentration. To identify and quantify geochemical reactions in the environment, laboratory studies are needed to determine fractionation factors for certain processes at varying reaction conditions. However, fractionation factors for many geochemical reactions involving Sb are still poorly known.

Kinetic isotope effects are those that occur predominantly in reactions that are far from equilibrium, as often occurs with redox reactions.[10] If a simple, single-step reaction with no back-reaction occurs, the light isotope tends to react faster compared to the heavy isotope due to differences in the isotope chemical properties. Therefore, the product of the reaction will be enriched in the faster reacting lighter isotope and the remaining reactant will be enriched in the heavy isotope. However, some redox reactions involve multiple steps with back-reaction that promotes isotopic equilibrium between steps. The difference between the reactant and product isotope ratios, or fractionation factor, is associated with a chemical reaction or process. The fractionation factor is represented by $\alpha = R_{product}/R_{reactant}$ or $\varepsilon = (\alpha - 1) * 1000‰ \approx \delta\,^{123}Sb_{product} - \delta\,^{123}Sb_{reactant}$ to show the direction and magnitude of fractionation.

The natural variation of $^{123}Sb/^{121}Sb$ has been shown to be large enough that it could be applied as a geochemical tracer.[11–13] Heavily Sb contaminated rain, groundwater, leachate, and spring water samples collected from the Xikuangshan Sb mine in China have shown isotopic variations from -0.11‰ to 0.27‰.[11] Another study characterized the natural isotopic variations of Sb in seawater, mantle-derived rocks, various environmental samples, deep-sea sediments and

hydrothermal sulfides from deep-sea vents.[13] Environmental samples including contaminated stream sediments and soil showed a range in isotopic variation of 0.45‰.[13] Hydrothermal sulfides from deep-sea vents exhibited the largest range in isotopic variation of 1.8‰, which was attributed to different Sb sources and the occurrence of low-temperature reduction.[13] A recent study by Resongles et al. (2015) found that two rivers in France, draining different mining sites, exhibited varying isotopic compositions. In all samples, Sb(V) was the only species detected in agreement with Sb speciation in natural oxic waters. Overall, the natural isotopic compositions ranged from -0.06‰ to 0.11‰ in the upper Orb River and from 0.23‰ to 0.83‰ in the Gardon River watershed.[12] A groundwater sample from the Dourdon and Gardon Sb-rich alluvial aquifer was enriched in the heavy isotope relative to a stream sample nearby.[12] This could indicate the isotopic composition of the natural Sb source, or the biogeochemical process of Sb reduction in the groundwater system.

Previous studies have shown that the reduction of Sb(V) by KI and ascorbic acid produced a fractionation of -0.55‰.[13] Given the limited experiments and narrow experimental conditions, the data for the isotopic fractionation induced by Sb(V) reduction is incomplete. The equilibrium isotopic fractionations ($\Delta^{123}Sb_{aqueous\text{-}adsorbed}$) for the adsorption of Sb onto goethite and illite at circumneutral pH was 0.34‰ and 0.25‰, respectively, where the adsorbed Sb is enriched in the light isotope.[14] The adsorption of Sb onto Fe (oxyhydr)oxides (ferrihydrite, hematite, and goethite) revealed $\Delta^{123}Sb_{aqueous\text{-}adsorbed}$ of 0.49 ± 0.004‰, 1.12 ± 0.006‰, and 1.14 ± 0.05‰, respectively.[15] While the adsorption of Sb(V) onto aluminum oxides did not produce any Sb equilibrium isotopic fractionation.[16] Since adsorption of Sb fractionates the isotopes in the same direction and magnitude as reduction, it has the potential to complicate the identification of redox-driven

isotopic fractionation in natural systems. If both Sb adsorption and reduction were occurring, adsorption could cause a significant overestimation of the Sb(V) reduction extent.[14]

In this study, we present results from controlled laboratory experiments that quantified the isotopic fractionation associated with the reduction of Sb(V) to Sb(III) by sulfide in environmentally relevant conditions. This study improves upon previously established Sb(V)-Sb(III) separation methods by increasing the recovery of Sb(III) from 85% to 100%. We also discuss the potential influence of reaction rate and reaction mechanism on fractionation and implications for the application of Sb isotopes in natural systems.

2. MATERIALS AND METHODS

2.1. Reagents and Standards

All solutions were prepared with ultrapure water (18.2 MΩ-cm) purified with a Millipore Milli-Q Integral system (Merck Millipore, USA). Ultra-pure HCl and HNO_3 were made by sub-boiling distillation of Certified ACS Plus concentrated HCl (Fisher Chemical) and Certified ACS Plus concentrated HNO3 (Fisher Chemical) using a Savillex DST-1000 Acid Purification System. Savillex PFA vials, polypropylene columns, glassware, pipette tips, and Nalgene LDPE bottles were cleaned with 8 M HNO_3 and 6 M HCl by soaking them overnight and rinsing them in Milli-Q water.

A solution that reduced Sb(V) and/or preserved Sb(III) consisted of 5% (m/v) KI (Certified ACS, Fisher Chemical) and 5% (m/v) ascorbic acid (Certified ACS, Fisher Chemical) and was prepared daily. A 0.2% (m/v) $NaBH_4$ (98% purity, Acros Organics) and 0.2% (m/v) NaOH (Fisher Chemical) solution was prepared daily for the hydride generation system. The 8.2 nMSb bracketing standard, abbreviated below as the "AOA" standard, was diluted daily from a concentrated Sb_2O_3 stock (Acros Organics, CAS 1309-64-4, lot AO312974) in 2 M HCl and 0.05%

(m/v) KI/ascorbic acid reducing agent. The 8.2 nM secondary standard, FUCA15b, was diluted daily from a concentrated stock in 2 M HCl and 0.05% (m/v) KI/ascorbic acid reducing agent. The bracketing standard and secondary standard were allowed to reduce for at least 3 hours before use in hydride generation.[17] An 8.2 mM Sb(III) stock solution was made daily from Sb_2O_3 (Acros Organics, CAS 1309-64-4, lot AO312974) in 2 M HCl and 0.02% (m/v) ascorbic acid for column purification. An 8.2 mM Sb(V) stock solution was prepared from $KSb(OH)_6$ (>94%, Alfa Aesar) in Milli-Q water for column purification and reduction experiments. A 1 mM Sb(V) solution for anoxic experiments was made by diluting the 8.2 mM Sb(V) stock solution in water under anaerobic conditions by degassing with N_2 (Airgas, Ultra High Purity). A 50 mM sulfide solution was made daily by dissolving $Na_2S•9H_2O$ (98% purity, Acros Organics) in water and storing it in a septum bottle with an N_2 headspace.

The media for the reduction experiments were prepared using various buffers. For pH 8 and 7 experiments, a 0.10 M Tris(hydroxymethyl)aminomethane-HCl buffer was used. The Tris(hydroxymethyl)aminomethane-HCl buffer was used for pH 6 experiments at a concentration of 0.15 M. For pH 5 experiments, a 0.10 M sodium acetate (anhydrous, 99% purity, Thermo Scientific)/acetic acid (HPLC grade, Fisher Chemical) buffer was used. For pH 1 experiments, a 0.5 M HCl matrix was used.

2.2. Sb(V) Sulfide Reduction Experimental Set-up

The anoxic batch experiments were carried out in degassed 160 mL serum bottles with thick butyl rubber stoppers and 100 mL of appropriate buffer media. Sb(V) and sulfide were added to each serum bottle until concentrations of 0.008 mM to 0.01 mM Sb(V) and 0.009 to 6 mM sulfide was reached. All Sb(V) and sulfide solutions were added from anoxic stock solutions by N_2-purged syringes and needles. During addition of Sb(V) and sulfide, the serum bottles were

shaken vigorously by hand to ensure complete mixing. All batch experiments were performed in duplicate.

After amendment with the appropriate Sb(V) and sulfide concentrations, the batch experiments were stored in the dark at 25°C. The pH 5 to 8 batch experiments were sampled by N_2-purged syringes at various intervals for Sb concentrations and isotopes. In the pH 1 experiment, varying extents of Sb(V) reduction was induced in a series of five identical serum bottles containing 8.2 μM Sb(V) and 9.2 μM, 11.2 μM, 13.6 μM, 17.6 μM, or 22.2 μM sulfide. These five bottles were sampled at 20 days when all of the sulfide was consumed and a stoichiometric amount of Sb(V) was reduced. Before withdrawal of a given sample volume, an equal volume of N_2 was added to the serum bottle to maintain positive pressure. At each sampling time, 1.67 mL sample was withdrawn from the serum bottle and filtered by a 0.2 μm nylon filter (Fisherbrand) into a 10 mL amber glass vial that had been previously stoppered and purged for 10 minutes to remove O_2. The samples in the amber glass vials were then purged with N_2 for 45 minutes to remove the dissolved sulfide as $H_2S(g)$. This was done to prevent additional reduction of Sb(V) by sulfide after sampling. To the purged samples, 0.040 mL of 1% (m/v) ascorbic acid and 0.288 mL of concentrated HCl was added to attain 1.5 M HCl and 0.02% ascorbic acid. The aqueous Sb(V) was then separated from aqueous Sb(III) using anion exchange.

For each batch experiment combination, a sulfide-absent control experiment and a Sb-absent blank experiment was carried out. The Sb(V) control experiments mimicked the Sb(V) concentration of their respective batch experiment but received no sulfide. This was done to monitor adsorption of Sb(V) on the serum bottles and unintended reduction of Sb(V) by the media. The blank experiments mimicked the sulfide concentration of their respective batch experiment

but received no Sb(V). This was done to determine any Sb(V) contamination in the media, sulfide, or experimental set-up process.

2.3. Sb Anion Exchange Purification

An anion exchange procedure adapted from Łukaszczyk and Zyrnicki[18], was used to separate Sb(V) and Sb(III). 1.5 mL of Eichrom 1x8 anion exchange resin (100-200 mesh, chloride form) was loaded into 10 mL acid-cleaned Bio-Rad Poly-prep polypropylene columns. The resin was then cleaned with 20 mL Milli-Q water, 10 mL of 1.0 M NaOH, 30 mL Milli-Q water, and conditioned with 10 mL of 1.5 M HCl in 0.02% (m/v) ascorbic acid. Each sample was acidified to 1.5 M HCl and 0.02% (m/v) ascorbic acid 1 hour prior to purification. The ascorbic acid acts as a preservative for Sb(III) and must be added before the HCl, which may contain traces of oxidants, to enable complete recovery of both Sb(III) and Sb(V). The Sb(V) fraction was eluted with 10 mL of 1.5 M HCl in 0.02% (m/v) ascorbic acid while the Sb(III) fraction remained adsorbed to the resin. Next, the Sb(III) fraction was eluted with 10 mL of 0.05M HCl. This is a modification from earlier versions of this procedure that called for elution with pure water. During this work it was found that elution with pure water led to incomplete recovery of Sb(III). Resin was successfully re-used after cleaning with 5 mL of 4 M HCl and 30 mL of 0.1 M HCl.

Complete column recovery of Sb(III) and Sb(V) was confirmed using a mixed standard of 1000 ng Sb(III) from Sb_2O_3 and 1000 ng Sb(V) from $KSb(OH)_6$. The recovery of Sb(V) was 100 ± 5% (n=4, 2σ) and the recovery for Sb(III) was 100 ± 6% (n=4, 2σ). The anion exchange procedure blank for Sb(V) was 6 ± 2 ng (n=5); it was 4 ± 3 ng (n=3) for Sb(III). For Sb(V) this is 0.08% of the smallest sample mass, and for Sb(III) this is 0.07% of the smallest sample mass.

2.4. Sb Concentration Measurements

Sb concentrations were measured on a Thermo Scientific™ iCAP™ Q ICP-MS to monitor reduction experiments and determine dilution factors needed for isotope measurements. All samples and standards were in a matrix of 2% HNO_3 and 0.2 M HCl. To eliminate Sb memory effects within the peristaltic tubing, a rinse of 2% HNO_3 and 0.2 M HCl flushed the system for 2 minutes between samples. An internal standard containing 87.1 nM ^{115}In was added to all samples and standards on-line to correct for instrumental drift and matrix effects. ^{123}Te was monitored to identify any Te interference. The limit of detection was 0.08 nM, and the limit of quantification was 0.8 nM. The long-term precision for replicate measurements was ± 5% (n=20, 2σ). The NIST SRM 1643f standard (trace elements in water solution) was measured within 7% of the certified Sb value at 491.0 ± 16.4 nM (n=6, 2σ).

2.5. Sb Isotope Measurements

Sb isotope ratios were measured using a Nu Plasma MC-ICP-MS instrument (Nu Instruments, UK) coupled to a hydride generation system at the University of Illinois Urbana-Champaign. Samples and standards were reduced completely to Sb(III) by a matrix of 2 M HCl and 0.05% (m/v) KI and ascorbic acid. The reduction to Sb(III) is important because the production of the H_3Sb(g) hydride is incomplete for Sb(V). The reduced sample was then reacted with 0.2% (w/v) $NaBH_4$ (stabilized by 0.2% (w/v) NaOH) on-line to form the Sb hydride for isotopic measurement. Samples and standards were measured at ca. 8.2 nM to produce a signal of 3.0 V – 5.0 V on ^{123}Sb. The system was rinsed for 4 minutes (1 minute in 4 sequential rinse buckets) with 2 M HCl and 0.05% (m/v) KI and ascorbic acid before every sample or standard.

^{121}Sb and ^{123}Sb were measured simultaneously, along with ^{122}Sn, ^{122}Te, ^{123}Te, and ^{126}Te for interference corrections. A sample-standard bracketing approach was used to correct for drift in the instrumental mass bias. As no certified isotopic standard exists for antimony, an in-house

isotope standard (AOA) was used as the bracketing standard. The $^{123}Sb/^{121}Sb$ variations were expressed as per mil deviations from the AOA standard using $\delta^{123}Sb$ defined as:

$$\delta^{123}Sb = \left(\frac{\frac{^{123}Sb}{^{121}Sb}_{sample} - \frac{^{123}Sb}{^{121}Sb}_{std}}{\frac{^{123}Sb}{^{121}Sb}_{std}} \right) * 1000‰ \quad (1)$$

Drift of the in-house bracketing standard followed a consistent linear trend and was typically less than 0.2‰ from the initial measurement over a 12-hour run. A secondary in-house, fractionated standard, FUCA15b (-0.76 ± 0.06‰), was measured every 4 samples to monitor the external correction. All samples were measured three times, with the replicates spread out over the run, to ensure the measurement was independent of the instrument conditions. Isobaric interference by ^{123}Te was corrected for by monitoring ^{126}Te and applying the following correction:

$$\frac{^{123}Sb}{^{121}Sb}(corrected) = \frac{^{123}Sb}{^{121}Sb} - \frac{\frac{^{126}Te}{^{121}Sb}}{RTe * \frac{M126^{\beta}}{M123}} \quad (2)$$

where R_{Te} is the $^{126}Te/^{123}Te$ ratio of naturally occurring Te, M_{126} is the atomic mass of ^{126}Te, M_{123} is the atomic mass of ^{123}Te, and β= 1.7562, the average mass bias exponent of our instrument. This correction was tested by adding Te to 8.2 nM Sb samples up to a 1:1 ratio, and no error was observed in the corrected $\delta^{123}Sb$ values. ^{120}Sn, ^{122}Sn, and ^{122}Te were monitored for interferences from $^{120}SnH+$, $^{122}SnH+$, and $^{122}TeH+$ because Sn and Te form volatile species in the hydride generator and are delivered to the plasma with the Sb. The average signals of ^{120}Sn, ^{122}Sn, and ^{122}Te contributed < 0.0000005% of an 8.2 nM signal on ^{123}Sb. Given the small signals for ^{120}Sn, ^{122}Sn, and ^{122}Te, no correction was applied.

The analytical uncertainties observed for unprocessed AOA and FUCA15b standards were ± 0.06‰ (n=185, 2σ) and ± 0.06‰ (n=55, 2σ), respectively. Anion exchange column-processed AOA standards and a 1 mM Sb(V) solution with the same matrix as the Sb(V) sulfide reduction

experiments were -0.02 ± 0.04‰ (n=6, 2σ) and -0.15 ± 0.08‰ (n=6, 2σ), respectively. This indicates no artificial fractionation from the anion exchange columns as the unprocessed AOA standard and 1 mM Sb(V) standard were 0‰ and -0.15‰, respectively. The Sb signal intensity (^{121}Sb and ^{123}Sb) measured for anion exchange column-processed blanks prepared for analysis following sample procedures contained less than 2% of the total Sb in a sample. The precision for duplicate preparations of a sample or standard in the experimental matrix was 0.06‰ (n=10, 2σ) and was calculated by:

$$2\sigma = 2 \cdot \sqrt{\frac{\sum_{i=1}^{n}(i_a - i_b)^2}{2 \cdot n}} \quad (3)$$

where i_a and i_b are the duplicate measurements and n is the number of duplicate pairs.

2.6. Rayleigh Distillation Model

A Rayleigh distillation model was used to extract isotopic fractionation factors from the data. A Rayleigh model assumes the system is closed and well-mixed, and the product does interact with the reactant in any way that alters isotope ratios. The isotopic composition of the remaining Sb(V) reactant is given by:

$$\delta^{123}Sb_{reactant} = \left(\delta^{123}Sb_o + 1000‰\right) f^{\alpha-1} - 1000‰ \quad (4)$$

where f= (C_t/C_o), C_t is the concentration as a function of time, and C_o is the initial concentration. Equation 4 was rearranged to the linear form as follows:[19]

$$\ln(\delta^{123}Sb_t + 1000‰) = (\alpha - 1)\ln(C_t) + [\ln(\delta^{123}Sb_o + 1000‰) - (\alpha - 1)\ln(C_o)] \quad (5)$$

Linear regression of $\ln(\delta^{123}Sb_t + 1000‰)$ vs $\ln(C_t)$ was used to find the best-fit line's slope and its uncertainty. The magnitude of isotopic fractionation, ε, was calculated from the slope using ε= (α-1) * 1000‰. Uncertainties for ε were calculated by multiplying the standard error of the slope by

two. The $\delta^{123}Sb_o$ used was calculated by averaging the $\delta^{123}Sb_o$ values of all experiments since the same Sb(V) stock was used in each experiment.

The isotopic composition of the accumulated product in a Rayleigh model is given by:

$$\delta^{123}Sb_{product} = \left(\delta^{123}Sb_o + 1000‰\right)\frac{1-f^{\alpha}}{1-f} - 1000‰ \quad (6)$$

The best-fit value of α was determined by trial and error fitting of the non-linear function to the data to maximize R_2:

$$R^2 = 1 - \left(\frac{SS_{residual}}{SS_{total}}\right) \quad (7)$$

where $SS_{residual}$ is the sum of the squared residuals, $\Sigma_i(y_i - \hat{y}_i)^2$ and SS_{total} is $\Sigma_i(y_i - \text{mean}(y))^2$. y_i is the experimental measurement value and $\hat{y}_i$ is the model value for a given extent of reaction. The α was adjusted until the best fit, or maximum R_2, was obtained for the accumulated product Rayleigh model.

2.7. Cross-contamination

Cross-contamination for the separation of Sb(V) and Sb(III) in the anion exchange procedure was determined by passing a Sb(III) standard through the column, analyzing the amount of Sb(V) recovered, and solving a mixing equation. A 1000 ng Sb(III) standard recovered 30 ng in the Sb(V) fraction. The Sb(V) fraction eluant, 1.5 M HCl in 0.02% (m/v) ascorbic acid, contributed 10 ng and the ion exchange procedure blank for Sb(V) contributed 6 ng. This leaves 14 ng or 1.4% of the Sb(III) fraction cross-contaminating the Sb(V) portion. All data were corrected to account for cross-contamination during separation before calculating the Rayleigh models.

3. RESULTS

3.1. Sb Species Concentrations

Experiments with Sb(V) and sulfide showed a decrease in Sb(V) concentrations and a simultaneous increase in Sb(III) concentrations as a function of time (Figure 1, Table S1). The time required for 50% of the initial Sb(V) to be reduced varied from 1 hour to 150 hours. The pH 1 experiment is not shown in figure 1 because it was not conducted as a time-series experiment (see methods), but initial Sb(V) concentrations decreased by 8%, 22%, 34%, 50%, and 88% for the series of five serum bottles. The difference in reaction rates between duplicate experiments is due to slight variations in sulfide concentrations of the stock solution during its preparation. Control experiments did not show a change in Sb(V) concentration or Sb(III) concentration with time within analytical uncertainty. For the pH 1, pH 5 and pH 6 experiments, the total aqueous Sb concentrations decreased from the initial concentration. This indicates Sb_2S_3 precipitation, as expected for lower pH.[20] However, a visible precipitate was only observed in the pH 1 and pH 5 experiment. For the pH 7 and pH 8 experiments, the total aqueous Sb concentration did not change from the initial concentration indicating no precipitation of Sb_2S_3. For the pH 1 condition, experiments were designed using an assumption that all Sb(III) in solution would precipitate, however 25% of the liquid phase Sb was present as Sb(III).

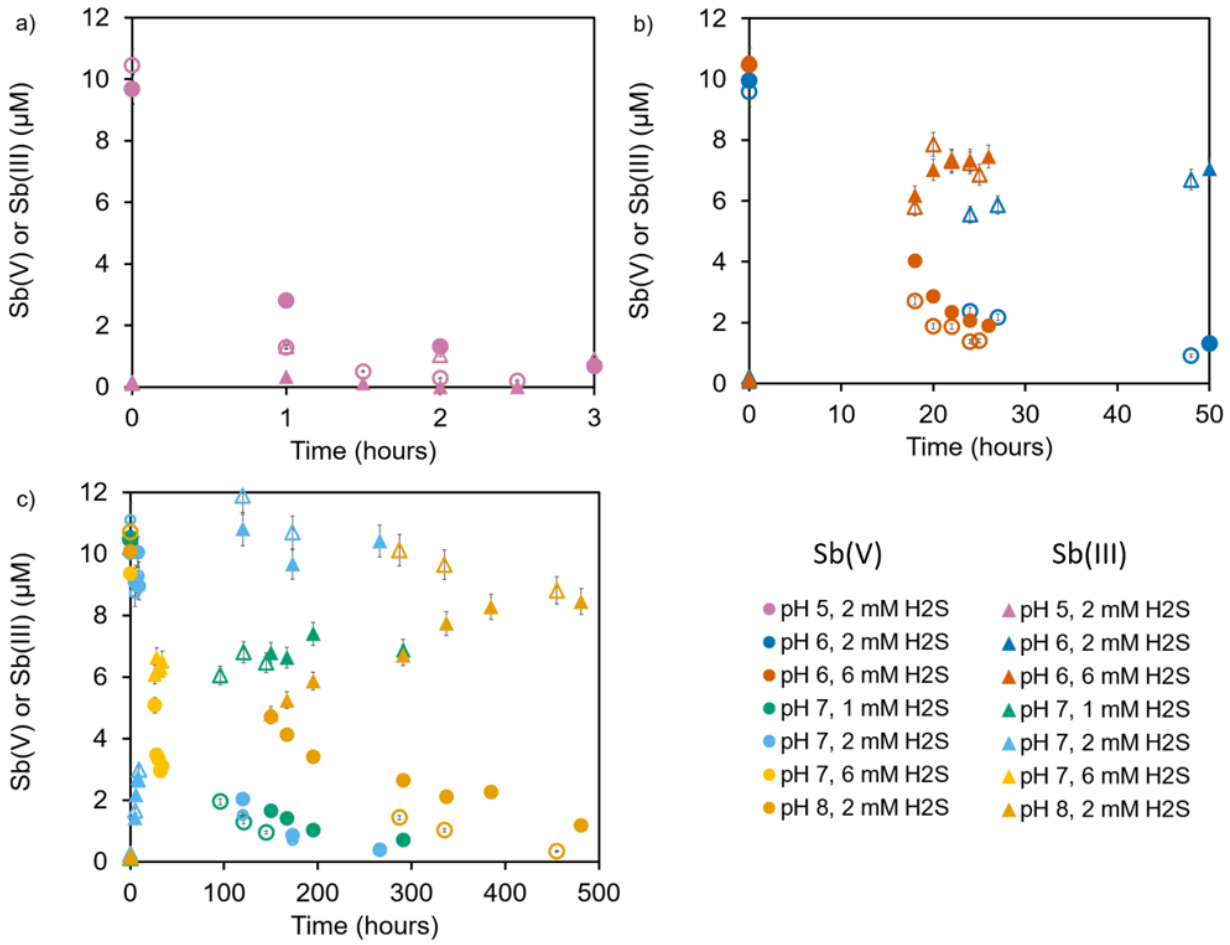

Figure 1. Time series for Sb(V) and Sb(III) concentrations of (a) the pH 5 and 2 mM sulfide experiment, (b) the pH 6 and 2 mM sulfide and the pH 6 and 6 mM sulfide experiments, and (c) the pH 7 and 1 mM sulfide, pH 7 and 2 mM sulfide, pH 7 and 6 mM sulfide, and the pH 8 and 2 mM sulfide experiments. The circle symbols represent Sb(V) concentrations and the triangle symbols represent Sb(III) concentrations. Open symbols of the same color represent duplicate experiments. Error bars represent the long-term analytical uncertainty of the iCAP-Q ICP-MS at ± 5% (2σ) which are sometimes smaller than the size of the symbols.

For the pH 5 to 8 experiments, a first-order rate law model fits all Sb(V) concentration data (Figure S1). The first-order rate constant ranged from 0.006 h^{-1} to 1.240 h^{-1} for all experiments (Table 1). The first-order rate law slope shows faster reaction rates with acidic pH and more sulfide, where the experiment with a pH of 5 and 2 mM sulfide was the fastest, and the experiment with a pH of 8 and 2 mM sulfide was the slowest. This is consistent with previous studies.[20]

Table 1. Average rate constant and magnitude of isotopic fractionation for various experimental conditions of pH and sulfide concentration.

Experiment	k (h^{-1})	$\varepsilon \pm 2\sigma$ (‰)
pH 1, 0.009 to 0.02 mM H_2S[a]	n.d.	-1.42 ± 0.04
pH 5, 2 mM H_2S	1.240	-0.46 ± 0.04
pH 6, 2 mM H_2S	0.045	-0.56 ± 0.08
pH 6, 6 mM H_2S	0.075	-0.48 ± 0.05
pH 7, 1 mM H_2S	0.014	-0.56 ± 0.04
pH 7, 2 mM H_2S	0.013	-0.49 ± 0.03
pH 7, 6 mM H_2S[a]	0.034	-0.53 ± 0.23
pH 8, 2 mM H_2S	0.006	-0.62 ± 0.04

[a]These had no duplicate experiment.

[b]n.d.= not determined

3.2. Sb(V) and Sb(III) Isotopes

At the beginning of the reaction, $\delta^{123}Sb$ of the reactant was on average -0.15‰ for all experiments except the pH 1 and 0.009 to 0.02 mM sulfide experiment which used a different Sb(V) solution with $\delta^{123}Sb$= -0.03‰. As the reaction progressed, the $\delta^{123}Sb$ of the remaining reactant became more positive (Figure 2). Most data points fit a Rayleigh model within their

uncertainty. The magnitude of isotopic fractionation ranged from -0.46 ± 0.04‰ to -1.42 ± 0.04‰. Duplicate experiments had ε values that were at most 0.09‰ different from each other. Sb(V) in the sulfide-absent control experiments did not deviate from the initial values, indicating that the experimental media and containers did not cause unintended isotopic fractionation. The sulfide-absent control experiments show that samples are not influenced by adsorption because the adsorption of Sb(V) to the glass bottle walls was negligible at less than 2% of the added Sb(V). In these controls, the added Sb(V) was 10.47 μM at T= 0 hours and was 10.28 μM at T= 455 hours.

The Sb(III) product was, in all experiments, enriched in the lighter isotope, relative to the Sb(V). Values of ε calculated using Sb(V) or Sb(III) data show no significant difference in isotopic fractionation between the two methods (Figure S2). In the pH 8 and 2 mM sulfide experiment, the Sb(V) data produced an ε of -0.62 ± 0.04‰ and the Sb(III) data produced an ε of -0.66 ± 0.08‰. Values of ε were calculated using both Sb(V) and Sb(III) for only the pH 8 and 2 mM sulfide experiment because the other experiments had complications with Sb(III) precipitation.

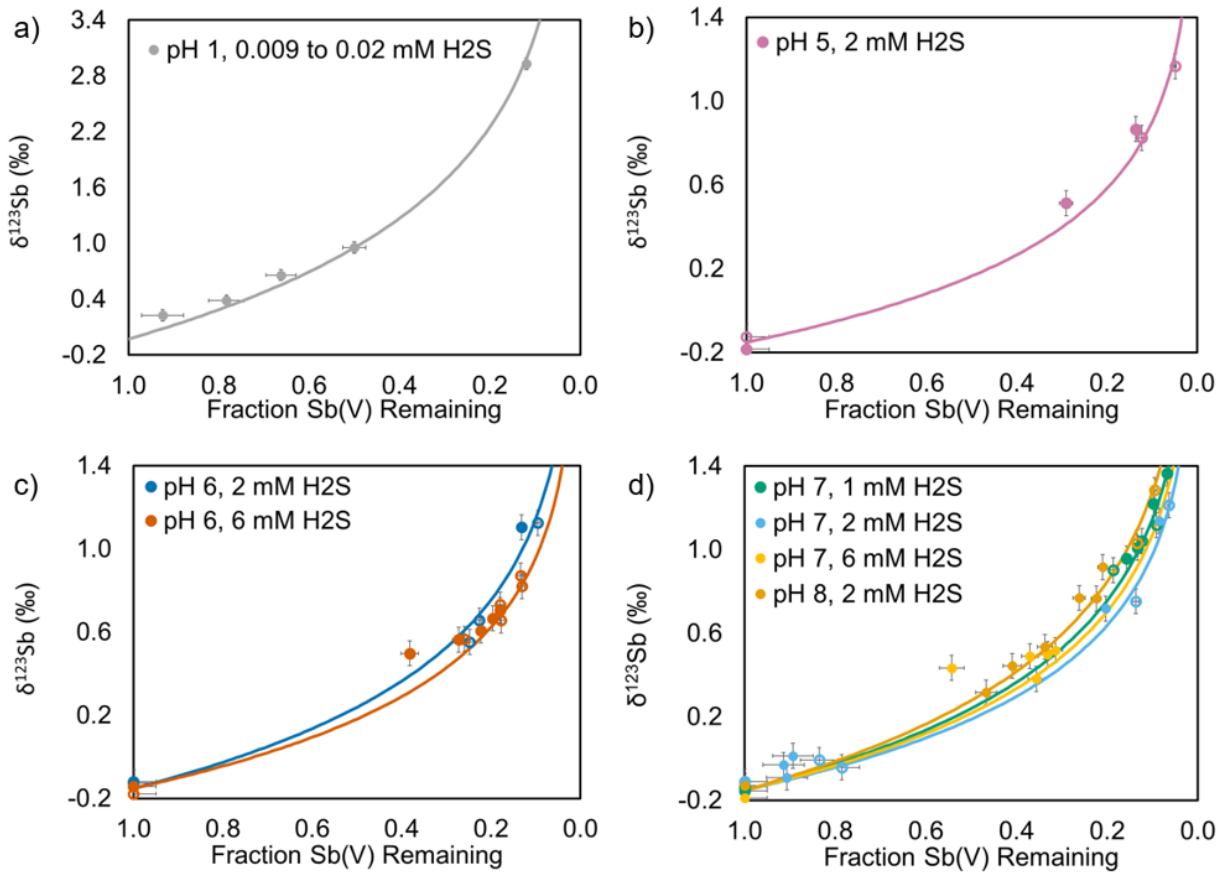

Figure 2. Sb isotope results and best-fit Rayleigh models of (a) the pH 1 and 0.01 mM sulfide experiment, (b) the pH 5 and 2 mM sulfide experiment, (c) the pH 6 and 2 mM sulfide and the pH 6 and 6 mM sulfide experiments, and (d) the pH 7 and 1 mM sulfide, pH 7 and 2 mM sulfide, pH 7 and 6 mM sulfide, and the pH 8 and 2 mM sulfide experiments . Colored circles represent individual data points, and the corresponding-colored lines represent Rayleigh fits of the data. Open symbols of the same color represent duplicate experiments. Error bars represent the long-term analytical uncertainty of the iCAP-Q ICP-MS at ± 5% (2σ) and the MC-ICP-MS at ± 0.06‰ (2σ) which are sometimes smaller than the size of the symbols.

4. DISCUSSION

4.1. Details of Rayleigh model fitting

In the later stages of several of the experiments, when most Sb(V) was reduced to Sb(III), the relatively high Sb(III):Sb(V) ratio in the solution, and the minor inclusion of Sb(III) in the separated Sb(V) fraction (see methods section) likely caused significant shifts in the δ^{123}Sb of the Sb(V) fraction. With an estimated 1.4% of the Sb(III) recovered in the Sb(V) fraction during anion exchange separation, the relatively low δ^{123}Sb of the Sb(III) significantly lowers δ^{123}Sb of the Sb(V) fraction. For this reason, only data points with an f greater than 0.05 were included in the calculation of ε. In isotope fractionation studies, typically data points with an f less than 0.1 are not used, but the correction for anion exchange separation mixing (see methods section) allowed for this.

Most of the data points fit Rayleigh models within analytical uncertainty, but some data points at earlier stages of the reaction are more positive than expected. Most notably, two pH 7 and 2 mM sulfide experiment points at f= 0.9 are 0.1‰ above the Rayleigh model. The pH 7 and 6 mM sulfide experiment also has an outlier at f= 0.5 that is 0.2‰ above the Rayleigh model. The pH 6 and 6 mM sulfide experiment has an outlier at f= 0.4 that is 0.2‰ above the Rayleigh model. The few data points that deviate from Rayleigh models in the early stages of the reaction could be due to changing conditions in our experiments as the reaction progresses. One potential changing condition is the decrease in sulfide concentrations which could lead to different Sb-S complexes. Alternatively, Sb(V) reduction by sulfide could be a multi-step redox reaction that does not fit a simple one-step Rayleigh model. A two-step kinetic process model that was used to fit Se isotope data from Se(IV) reduction experiments shows the same trend of isotope data above the Rayleigh model at the early stages of the reaction.[21] If our isotope data were fit to a two-step kinetic process model, the isotope fractionation would be dependent on the fraction of reactant remaining, and the isotope fractionation would be larger at the early stages of the reaction. However, the few data

points at early stages of the reaction that are more positive than expected do not cause large enough changes to the fractionation to warrant applying the two-step kinetic process model.

4.2. Implications of Sb_2S_3 precipitation

The experiments at pH 1, 5, and 6 precipitated some Sb(III) as Sb_2S_3 in the final product. In the pH 5 and 6 experiments, separation of aqueous Sb(V) from Sb(III) using anion exchange and the isotope measurement of only Sb(V) should allow for accurate extraction of ε from the data despite the partial conversion of Sb(III) to Sb_2S_3 precipitate. The close fit of the data to Rayleigh models indicates that isotopic fractionation for the reduction of Sb(V) to Sb(III) is kinetically controlled and the back-reaction of Sb(III) to Sb(V) is minimal. Accordingly, although Sb_2S_3 precipitation may involve Sb isotopic fractionation and therefore affect the δ^{123}Sb of Sb(III), the δ^{123}Sb of Sb(V) is not affected and reflects only the kinetic isotope effect occurring in the Sb(V) reduction reaction.

In contrast to the pH 5 and 6 experiments, the pH 1 experiment was designed using an assumption that all Sb(III) in solution would precipitate, and thus the measured solution would contain only Sb(V). Accordingly, Sb(III)-Sb(V) separation of dissolved Sb was not done and δ^{123}Sb was measured for total dissolved Sb. However, it was later discovered that for one sample at f= 0.78 that separated dissolved Sb(III) and Sb(V) using anion exchange, about 25% of the liquid phase Sb was present as Sb(III) that did not form an Sb_2S_3 precipitate. This was probably related to the very low (0.009 to 0.02 mM) starting sulfide concentration, and the fact that the experiment was designed to consume all the sulfide. With some of the Sb(III) remaining in solution, the measured δ^{123}Sb of the aqueous Sb was a mixture of Sb(V) and Sb(III). The admixture of isotopically light Sb(III) into the Sb(V) fraction is thus assumed to have led to lower measured δ^{123}Sb values, relative to the actual Sb(V) fraction. Accordingly, the ε value of -1.42‰ derived

from the pH 1 Rayleigh model should be viewed as a minimum value. The δ^{123}Sb value of the separated Sb(V) fraction at f= 0.78 was 0.84‰, and using this Sb(V) sample, the ε value was -3.55‰. However, this ε value was produced from only two samples which results in a large uncertainty. We chose not to pursue refinement of this experiment, as the pH is outside the range of essentially all earth environments. Nonetheless, the pH 1 experiment result provides a clear indication that isotopic fractionation generated by Sb(V) reduction by sulfide can be much larger than that observed in our experiments between pH 5 and pH 8.

4.3. Dependence of Sb Isotope Fractionation on Reaction Kinetics

The large difference between the ε value observed in the pH 1 and 0.009 to 0.02 mM sulfide experiment (-1.42‰) and the values observed in the experiments at pH 5 to 8 and sulfide concentrations between 1 to 6 mM experiments (-0.46‰ to -0.62‰) must be related to differences in the kinetics and/or mechanism of the reaction. Isotopic fractionation is controlled by changes to the local bonding environment of elements, and the changes in coordination and valence that accompany redox reactions often produce relatively strong isotopic fractionation.[22] During mass-dependent kinetic isotope effects, bonds with lighter isotopes have higher zero-point energies than bonds with heavier isotopes.[23] When a single-step reaction with no back reaction occurs, bonds involving lighter isotopes are more easily broken and the lighter isotopes react faster.[24] However, Sb(V) reduction by sulfide is a multi-step redox reaction that may involve ephemeral intermediate products and potential back-reaction. Back-reaction of individual steps may cause an approach toward isotopic equilibrium of those steps, whereas a dominantly forward-reacting step promotes a simple kinetic isotope effect for that step. The overall Sb(V) reduction reaction discussed here includes an Sb coordination change and transfer of two electrons from sulfide to Sb(V) to produce Sb(III), followed by the formation of an aqueous Sb(III)-S complex, Sb(III)-Cl complex, or Sb_2S_3

precipitate. According to theoretical models often used to understand isotopic fractionation induced by redox reactions, overall fractionation is the sum of the individual fractionations for all steps up to, and including, the rate-limiting step, even if later steps induce large fractionations.[23,25] For the Sb(V) reduction reaction, we do not know the reaction mechanisms nor which step is rate-limiting, but the coordination change between Sb(V) and Sb(III) complexes and the transfer of electrons from sulfide to Sb(V) are likely to be rate-limiting. Our observation of relatively large isotopic fractionation in the pH 1 experiment suggests that the rate-limiting step is relatively late in the reaction sequence and involves major bonding changes. In contrast, the relatively small fractionation observed in all the circumneutral experiments suggests that the rate-limiting step is relatively early, before the steps involving major bonding changes. Speculatively, this is caused by the very different Sb(V) speciation in the circumneutral experiments, with lower Cl^- and H^+ concentrations, and higher S(-II) concentrations.

In the Sb(V) reduction reactions of our experiments, the reactant and product species include Sb-O complexes, Sb-S complexes, and Sb-Cl complexes that have varying coordination geometries. The Sb-O complexes for the Sb(V) reduction reaction, $Sb(OH)_6^-$, $Sb(OH)_5$, and $Sb(OH)_3$, depend on pH. At a neutral pH of 7, the Sb(V) reduction reaction expected in the presence of dissolved sulfide can be written as $Sb(OH)_6^- + H_2S + H^+ \rightarrow Sb(OH)_3 + 1/8S_8(s) + 3H_2O$. In acidic pH's (< 5), $Sb(OH)_6^-$ dissociates to form a more reactive species, $Sb(OH)_5$.[20] At pH less than 5, the Sb(V) reduction reaction expected in the presence of dissolved sulfide can be written as $Sb(OH)_5 + H_2S \rightarrow Sb(OH)_3 + 1/8S_8(s) + 2H_2O$. The geometries of these Sb(V)-O and Sb(III)-O complexes, $Sb(OH)_6^-$, $Sb(OH)_5$, and $Sb(OH)_3$ are octahedral, trigonal bipyramidal, and trigonal pyramidal, respectively (Figure 3).

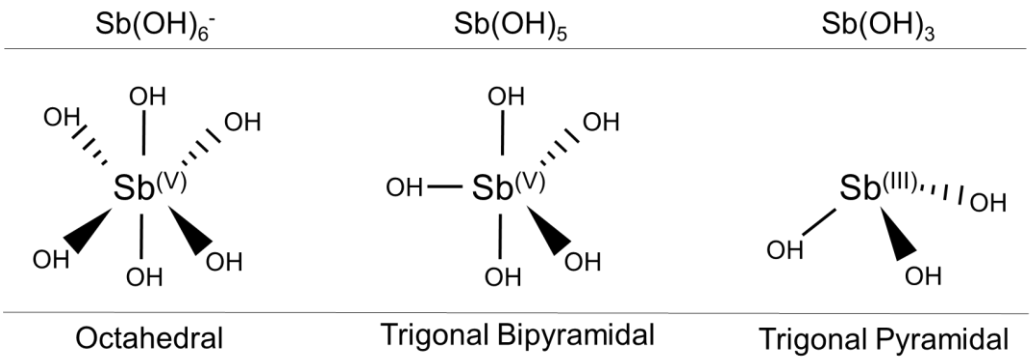

Figure 3. Geometries of common Sb(V) and Sb(III)-hydroxide complexes found in the environment drawn using Dashed-Wedged Line structure.[26–28] The straight lines illustrate bonds that are in the plane of the page, dashed lines show bonds that go into the page, and wedged lines illustrate bonds that come out of the page.

Sb(III) is able to form stable aqueous Sb(III)-S complexes such as $H_2Sb_2S_4$, $HSb_2S_4^-$, and $Sb_2S_4^{2-}$ when in the presence of high sulfide concentrations.[29–32] Since Sb(III)-S complexes, Sb(III)-Cl complexes, and Sb_2S_3 precipitates form after the rate-limiting step, their presence likely has no control on the isotope fractionation. For the pH 1 experiment with a matrix of 0.5 M HCl and low sulfide concentrations, we expect Sb(V) in the system was present as $Sb(OH)_3Cl_3^-$ with minor amounts of $Sb(OH)_2Cl_4^-$ and $Sb(OH)_4Cl_2^-$ [33], and the Sb(III) is present as $SbCl_4^-$.[34]

Based on existing knowledge of Sb aqueous speciation, we suggest that the major species involved in our experiment are as follows: At pH 1, $Sb(OH)_3Cl_3^-$ is reduced to $SbCl_4^-$. At pH 5, $Sb(OH)_5$ is reduced to $Sb(OH)_3$, $H_2Sb_2S_4^-$ is formed, and Sb_2S_3 is precipitated. At pH 6, $Sb(OH)_6^-$ is reduced to $Sb(OH)_3$, $HSb_2S_4^-$ is formed, and Sb_2S_3 is precipitated. At pH 7, $Sb(OH)_6^-$ is reduced to $Sb(OH)_3$ and $HSb_2S_4^-$ is formed. At pH 8, $Sb(OH)_6^-$ is reduced to $Sb(OH)_3$ and $HSb_2S_4^-$ or $Sb_2S_4^{2-}$ are formed. The known variation in the Sb product and reactant species present in our various experiments causes differences in Sb coordination and, therefore, Sb bond energy changes

of the overall reaction. The characteristics of ephemeral, intermediate species that may control the reaction kinetics (i.e., rate-limiting step(s)), are poorly known, but we expect them to vary as availability of S^{2-}, Cl^{-}, and H^{+} vary.

4.4. Dependence of Sb Isotope Fractionation on Experimental Conditions and Reaction Rate

The reaction rates of our pH 5 to 8 experiments, which have excess sulfide present and fit pseudo first-order rate laws, depended on pH and sulfide concentration in accordance with a previous kinetic rate study.[20] The reaction rate is faster at lower pH and higher sulfide concentrations. The one exception to this rule is the comparison between the pH 7 and 1 mM sulfide experiment and the pH 7 and 2 mM sulfide experiment, which have rate constants that are the same within analytical uncertainty. This disparity is likely due to uncertainty in the concentrations of the sulfide stock solutions, which are made fresh each day and are prone to exposure to air and/or loss of sulfide as the stock is degassed.

Previous studies have shown that faster or more thermodynamically favorable reactions tend to generate less isotopic fractionation.[35] This linear free energy relationship between the magnitude of fractionation and reaction rate becomes observable when isotopic fractionation is kinetically controlled.[36] For our fastest reaction rate in the pH 5 and 2 mM sulfide experiment, the smallest fractionation of -0.46 ± 0.04‰ was observed. For our slowest reaction rate in the pH 8 and 2 mM sulfide experiment, the greatest fractionation of -0.62 ± 0.04‰ occurred. For the pH 5 and 2 mM sulfide experiment and the pH 8 and 2 mM sulfide experiment, our results are consistent with a small rate effect. However, for the other five experiments, variations in ε do not exceed the uncertainties. Overall, the magnitude of isotopic fractionation appears to have a slight dependence on reaction rate, but it is so small that it will have little impact on practical applications of Sb

isotopes. Notably, in the two pairs of experiments that differed only in sulfide concentrations, ε did not depend significantly on sulfide concentration in the 2 mM to 6 mM range.

4.4. Relevance in Natural Systems

When anoxic conditions are reached in soil, deep marine sediments, or aquifers, sulfur geochemistry can be a dominant control on the redox reactions that occur. Few electron donors can reduce Sb(V), and sulfide may be the most important abiotic reduction mechanism for Sb(V) in natural systems. The reduction of Sb(V) can cause immobilization of Sb. In sulfidic environments at low pH, such as acid mine drainage, most reduced Sb will precipitate as Sb_2S_3.[20] However, in sulfidic environments at circumneutral pH, such as aquifers and rivers, Sb(III) is more likely to form aqueous Sb-S complexes that do not precipitate and allow Sb to exist in mobile forms. More generally, the redox state of Sb controls its geochemical properties, and the understanding of Sb isotopic fractionation provided by our experiments improves the ability to understand Sb biogeochemical cycling in past and present systems.

Sulfide also exists in past and present deep marine and sedimentary environments.[37–39] In the geologic past, parts of the ocean that were isolated or stagnant were euxinic, or had high concentrations of sulfide and no O_2.[37] During this time, when sulfate was reduced to sulfide at the sediment-water interface, trace elements like Sb underwent deposition as sulfide minerals which were preserved in the rock record. Knowledge of Sb isotope shifts could therefore be used to infer pale-redox conditions in the rock record similar to other studies using elements such as Cr, Mo, and U.[40–42]

Our results provide some initial estimates of the magnitude of Sb isotope fractionation induced by sulfide-driven Sb(V) reduction in natural systems, but a more complete understanding will require additional work. Our array of experiments at pH values between 5 and 8 and sulfide

concentrations between 1 and 6 mM suggest that sulfide-driven Sb(V) reduction is approximately 0.5‰ in natural environments under this range of conditions. However, it seems possible that, in environments with lower sulfide concentrations, or marine environments with high Cl^- concentrations, changes in reaction kinetics and Sb speciation could lead to fractionation similar to that observed in our low-sulfide, high chloride, pH 1 experiment, at over 1.0‰. Overall, the results of this study should be viewed as an initial survey; a fuller understanding of the controls on isotopic fractionation during Sb(V) reduction by sulfide is needed to determine fractionation factors for various natural settings.

If the small isotope fractionation we observed for Sb(V) reduction by sulfide in our circum-neutral pH experiments turns out to occur widely in nature, our ability to interpret Sb isotope shifts as indicators of redox reactions may be limited. Sb adsorption onto goethite and illite induces δ^{123}Sb shifts of about 0.3‰[14]; this is more than half of the fractionation we observed for reduction. Interpreting natural δ^{123}Sb values that were influenced by both adsorption and reduction is most successful when the fractionation for one process is significantly larger than the other processes. Before Sb stable isotopes can be used to track geochemical processes in the environment, a wide variety of laboratory studies are needed for many Sb processes. These geochemical processes should include oxidation of Sb(III) by O_2 and Fe(III), precipitation of Sb(III), and reduction of Sb(V) by microorganisms.

5. CONCLUSIONS

In our experiments, Sb(V) was reduced by sulfide at rates that were similar to those observed in previous studies where reduction was fastest at lower pH and greater concentrations of sulfide. In several experiments carried out at pH 5 to 8 with 1 to 6 mM sulfide, isotopic fractionation ranged from -0.46 ± 0.04‰ to -0.62 ± 0.04‰. In one experiment at pH 1.0 and 0.009

to 0.02 mM sulfide, ε was much larger, at -1.42 ± 0.04‰. As is observed with redox reactions in many other elements, the reaction is a complex, multi-step, kinetically controlled process in which the isotopic fractionation depends on the conditions. Variables such as Sb speciation, reaction mechanism, and reaction rate appear to control the magnitude of Sb isotopic fractionation, but a predictive understanding of those controls could not be extracted from our results. However, there appears to be a small reaction rate effect; our experiment with the fastest reaction rate generated the least amount of fractionation. Fractionation was not strongly sensitive to sulfide concentration. While our experiments contained low concentrations of Sb and low to high concentrations of sulfide at acidic and circumneutral pH, additional work is needed to better understand the controls on the fractionation in natural systems.

Improving our knowledge of Sb isotope shifts expected in systems that contain sulfide may lead to successful use of δ^{123}Sb to track immobilization of toxic Sb via reduction reactions. For example, Sb isotope data could provide evidence for Sb(V) reduction in an Sb-contaminated groundwater plume. Similarly, Sb isotope shifts in ancient rocks may provide evidence for changes in the global Sb redox cycle caused by evolving atmospheric O_2, marine anoxic or euxinic events. However, adsorption of Sb has been shown to fractionate Sb isotopes significantly[14,15] and this may complicate interpretation of Sb isotope data if the small fractionations we observed are found to occur widely in nature.

ASSOCIATED CONTENT

Table of Sb concentration and isotope data for all experiments; first-order rate law slopes; Rayleigh model for pH 8 and 2 mM experiment using Sb(V) and Sb(III) data (PDF).

Corresponding Author

*Hannah J. Veldhuizen- Department of Earth Science and Environmental Change, University of Illinois Urbana-Champaign, Champaign, IL, 61801, USA; Email: hjv3@illinois.edu

Present Addresses

†AECOM, Milwaukee, WI 53212, USA

Author Contributions

The manuscript was written through contributions of all authors. All authors have given approval to the final version of the manuscript. ‡These authors contributed equally.

Funding Sources

This material is based upon work supported by the National Science Foundation Graduate Research Fellowship under Grant No. (2146756). Any opinion, findings, and conclusions or recommendations expressed in this material are those of the authors(s) and do not necessarily reflect the views of the National Science Foundation.

REFERENCES

(1) ATSDR. Toxicological Profile for Antimony and Compounds. In *ATSDR's Toxicological Profiles*; 2002. https://doi.org/10.1201/9781420061888_ch32.

(2) Miao, Z.; Brusseau, M. L.; Carroll, K. C.; Carreón-Diazconti, C.; Johnson, B. Sulfate Reduction in Groundwater: Characterization and Applications for Remediation. *Environ. Geochem. Health* **2012**, *34* (4), 539–550. https://doi.org/10.1007/s10653-011-9423-1.

(3) Li, J.; Wang, Q.; Oremland, R. S.; Kulp, T. R.; Rensing, C.; Wang, G. Microbial Antimony Biogeochemistry: Enzymes, Regulation, and Related Metabolic Pathways. *Applied and Environmental Microbiology*. 2016. https://doi.org/10.1128/AEM.01375-16.

(4) Fu, Z.; Wu, F.; Amarasiriwardena, D.; Mo, C.; Liu, B.; Zhu, J.; Deng, Q.; Liao, H. Antimony, Arsenic and Mercury in the Aquatic Environment and Fish in a Large Antimony Mining Area in Hunan, China. *Sci. Total Environ.* **2010**. https://doi.org/10.1016/j.scitotenv.2010.04.031.

(5) Herath, I.; Vithanage, M.; Bundschuh, J. Antimony as a Global Dilemma: Geochemistry, Mobility, Fate and Transport. *Environmental Pollution*. 2017. https://doi.org/10.1016/j.envpol.2017.01.057.

(6) Kulp, T. R.; Miller, L. G.; Braiotta, F.; Webb, S. M.; Kocar, B. D.; Blum, J. S.; Oremland, R. S. Microbiological Reduction of Sb(V) in Anoxic Freshwater Sediments. *Environ. Sci. Technol.* **2014**. https://doi.org/10.1021/es403312j.

(7) Wang, L.; Ye, L.; Yu, Y.; Jing, C. Antimony Redox Biotransformation in the Subsurface: Effect of Indigenous Sb(V) Respiring Microbiota. *Environ. Sci. Technol.* **2018**. https://doi.org/10.1021/acs.est.7b04624.

(8) Yang, Z.; Hosokawa, H.; Sadakane, T.; Kuroda, M.; Inoue, D.; Nishikawa, H.; Ike, M. Isolation and Characterization of Facultative-Anaerobic Antimonate-Reducing Bacteria. *Microorganisms* **2020**. https://doi.org/10.3390/microorganisms8091435.

(9) Berna, Emily C., Johnson, Thomas, M., Makdisi, Richard, S., and Basu, A. Cr (VI) Reduction in Groundwater : A Detailed Time-Series Study of a Point-Source Plume. *Environ. Sci. Technol.* **2010**, *44* (3), 1043–1048.

(10) Dauphas, N.; Watkins, J. M. Non-Traditional Stable Isotopes: Retrospective and Prospective. **2017**, *82*, 1–26.

(11) Li, S.; Deng, Y.; Zheng, H.; Liu, X.; Tang, P.; Zhou, J.; Zhu, Z. A New Purification Method Based on a Thiol Silica Column for High Precision Antimony Isotope Measurements. *J. Anal. At. Spectrom.* **2021**, *36* (1), 157–164. https://doi.org/10.1039/d0ja00367k.

(12) Resongles, E.; Freydier, R.; Casiot, C.; Viers, J.; Chmeleff, J.; Elbaz-Poulichet, F. Antimony Isotopic Composition in River Waters Affected by Ancient Mining Activity. *Talanta* **2015**, *144*, 851–861. https://doi.org/10.1016/j.talanta.2015.07.013.

(13) Rouxel, O.; Ludden, J.; Fouquet, Y. Antimony Isotope Variations in Natural Systems and Implications for Their Use as Geochemical Tracers. *Chem. Geol.* **2003**. https://doi.org/10.1016/S0009-2541(03)00121-9.

(14) Wasserman, N. Tellerium, Antimony, and Selenium Isotopes and Indicators of Elemental Mobility, Ph.D Dissertation, University of Illinois Urbana-Champaign, 2020.

(15) Zhou, W.; Zhou, J.; Feng, X.; Wen, B.; Zhou, A.; Liu, P.; Sun, G.; Zhou, Z.; Liu, X. Antimony Isotope Fractionation Revealed from EXAFS during Adsorption on Fe (Oxyhydr)Oxides. *Environ. Sci. Technol.* **2023**, *57* (25), 9353–9361. https://doi.org/10.1021/acs.est.3c01906.

(16) Zhou, W.; Zhou, A.; Wen, B.; Liu, P.; Zhu, Z.; Finfrock, Z.; Zhou, J. Antimony Isotope Fractionation during Adsorption on Aluminum Oxides. *J. Hazard. Mater.* **2022**, *429* (November 2021), 128317. https://doi.org/10.1016/j.jhazmat.2022.128317.

(17) Asaoka, S.; Takahashi, Y.; Araki, Y.; Tanimizu, M. Preconcentration Method of Antimony Using Modified Thiol Cotton Fiber for Isotopic Analyses of Antimony in Natural Samples. *Anal. Sci.* **2011**, *27* (1), 25–28. https://doi.org/10.2116/analsci.27.25.

(18) Łukaszczyk, L.; Zyrnicki, W. Speciation Analysis of Sb(III) and Sb(V) in Antileishmaniotic Drug Using Dowex 1×4 Resin from Hydrochloric Acid Solution. *J. Pharm. Biomed. Anal.* **2010**, *52* (5), 747–751. https://doi.org/10.1016/j.jpba.2010.02.009.

(19) Scott, K. M.; Lu, X.; Cavanaugh, C. M.; Liu, J. S. Optimal Methods for Estimating Kinetic Isotope Effects from Different Forms of the Rayleigh Distillation Equation. *Geochim. Cosmochim. Acta* **2004**, *68* (3), 433–442. https://doi.org/10.1016/S0016-7037(03)00459-9.

(20) Polack, R.; Chen, Y. W.; Belzile, N. Behaviour of Sb(V) in the Presence of Dissolved Sulfide under Controlled Anoxic Aqueous Conditions. *Chem. Geol.* **2009**, *262* (3–4), 179–185. https://doi.org/10.1016/j.chemgeo.2009.01.008.

(21) Krouse, H. R.; Rashid, K. Selenium Isotopic Fractionation during Se032- Reduction to Seo and H2Se. *Can. J. Chem.* **1985**, *63*, 3195–3199.

(22) Johnson, T. M.; Druhan, J. L.; Basu, A.; Jemison, N. E.; Wang, X.; Schilling, K.; Wasserman, N. L. *A Review of the Development of Cr, Se, u, Sb, and Te Isotopes as Indicators of Redox Reactions, Contaminant Fate, and Contaminant Transport in Aqueous Systems*; 2022. https://doi.org/10.1002/9781119595007.ch10.

(23) Schauble, E. A. Applying Stable Isotope Fractionation Theory to New Systems. *Rev. Mineral. Geochemistry* **2004**, *55*, 65–111. https://doi.org/10.2138/gsrmg.55.1.65.

(24) White, W. *Isotope Geochemistry*, 1st ed.; John Wiley & Sons, 2015.

(25) Hayes, J. M. Fractionation of Carbon and Hydrogen Isotopes in Biosynthetic Processes. *Stable Isot. Geochemistry* **2019**, *43* (March), 225–277. https://doi.org/10.1515/9781501508745-006.

(26) Pauling, L. The Formulas of Antimonic Acid and Antimonates. *J. Am. Chem. Soc.* **1933**, *55* (5), 1895–1900. https://doi.org/10.1021/ja01332a016.

(27) Baes, C.; Mesmer, R. *The Hydrolysis of Cations*; Wiley, 1976.

(28) Pitman, A. L.; Pourbaix, M.; de Zoubov, N. Potential-PH Diagram of the Antimony-Water System; Its Applications to Properties of the Metal, Its Compounds, Its Corrosion, and Antimony Electrodes. *J. Electrochem. Soc.* **1958**, *105* (6), 365–365.

(29) Krupp, R. E. Solubility of Stibnite in Hydrogen Sulfide Solutions, Speciation, and Equilibrium Constants, from 25 to 350°C. *Geochim. Cosmochim. Acta* **1988**, *52* (12), 3005–3015. https://doi.org/https://doi.org/10.1016/0016-7037(88)90164-0.

(30) Olsen, N. J.; Mountain, B. W.; Seward, T. M. Antimony(III) Sulfide Complexes in Aqueous Solutions at 30 °C: A Solubility and XAS Study. *Chem. Geol.* **2018**, *476* (November 2017), 233–247. https://doi.org/10.1016/j.chemgeo.2017.11.020.

(31) Wood, S. A.; Samson, I. M. Solubility of Ore Minerals and Complexation of Ore Metals in Hydrothermal Solutions. *Techniques in Hydrothermal Ore Deposits Geology*. Society of Economic Geologists January 1, 1998, p 0. https://doi.org/10.5382/Rev.10.02.

(32) Spycher, N. F.; Reed, M. H. As (III) and Sb(III) Sulfide Complexes: An Evaluation of Stoichiometry and Stability from Existing Experimental Data. *Geochim. Cosmochim. Acta* **1989**, *53* (9), 2185–2194. https://doi.org/10.1016/0016-7037(89)90342-6.

(33) Neumann, B. M. Antimony (V) Species in Hydrochloric Acid Solution. **1954**, No. V, 4–8.

(34) Milne, J. Spectrophotometric Studies on Sb(III) in Hydrochloric Acid Solutions. *Can. J. Chem.* **1975**, *53* (6), 888–893. https://doi.org/10.1139/v75-123.

(35) Joe-Wong, C.; Maher, K. A Model for Kinetic Isotope Fractionation during Redox Reactions. *Geochim. Cosmochim. Acta* **2020**, *269*, 661–677. https://doi.org/10.1016/j.gca.2019.11.012.

(36) Joe-Wong, C.; Weaver, K. L.; Brown, S. T.; Maher, K. Thermodynamic Controls on Redox-Driven Kinetic Stable Isotope Fractionation. *Geochemical Perspect. Lett.* **2019**, *10* (Ii), 20–25. https://doi.org/10.7185/geochemlet.1909.

(37) Olson, K. R.; Straub, K. D. The Role of Hydrogen Sulfide in Evolution and the Evolution of Hydrogen Sulfide in Metabolism and Signaling. *Physiology* **2016**, *31* (1), 60–72. https://doi.org/10.1152/physiol.00024.2015.

(38) Lyons, T. W.; Anbar, A. D.; Severmann, S.; Scott, C.; Gill, B. C. Tracking Euxinia in the Ancient Ocean: A Multiproxy Perspective and Proterozoic Case Study. *Annu. Rev. Earth Planet. Sci.* **2009**, *37*, 507–534. https://doi.org/10.1146/annurev.earth.36.031207.124233.

(39) Meyer, K. M.; Kump, L. R. Oceanic Euxinia in Earth History: Causes and Consequences. *Annu. Rev. Earth Planet. Sci.* **2008**, *36*, 251–288. https://doi.org/10.1146/annurev.earth.36.031207.124256.

(40) Archer, C.; Vance, D. The Isotopic Signature of the Global Riverine Molybdenum Flux and Anoxia in the Ancient Oceans. *Nat. Geosci.* **2008**, *1* (9), 597–600. https://doi.org/10.1038/ngeo282.

(41) Frei, R.; Gaucher, C.; Poulton, S. W.; Canfield, D. E. Fluctuations in Precambrian Atmospheric Oxygenation Recorded by Chromium Isotopes. *Nature* **2009**, *461* (7261), 250–253. https://doi.org/10.1038/nature08266.

(42) Kendall, B.; Brennecka, G. A.; Weyer, S.; Anbar, A. D. Uranium Isotope Fractionation Suggests Oxidative Uranium Mobilization at 2.50Ga. *Chem. Geol.* **2013**, *362*, 105–114. https://doi.org/10.1016/j.chemgeo.2013.08.010.

For Table of Contents Only